Available online at www.sciencedirect.com
SCIENCE DIRECT®

Journal of the European Ceramic Society 23 (2003) 1865–1873
www.elsevier.com/locate/jeurceramsoc

Chemical interactions between 3 mol% yttria-zirconia and Sr-doped lanthanum manganite

San Ping Jiang[a,*], Jin-Ping Zhang[b], Karl Föger[b]

[a]*Fuel Cells Strategic Research Program, School of Mechanical and Production Engineering, Nanyang Technological University, 50 Nanyang Ave., 639798, Singapore*
[b]*Ceramic Fuel Cells Limited, 170 Browns Road, Noble Park, Vic. 3174, Australia*

Received 12 January 2002; received in revised form 31 October 2002; accepted 8 November 2002

Abstract

The chemical interactions between porous $(La_{0.8}Sr_{0.2})MnO_3$ (LSM) film and 3 mol% yttria tetragonal zirconia (TZ3Y) substrate have been investigated over the temperature range of 1300–1500 °C in air. Two distinct reaction layers of fluorite-type cubic zirconia solid solution c-$(Zr,Mn,La,Y)O_2$ and lanthanum zirconate pyrochlore $(La,Sr)_2(Zr,Y)_2O_7$ were observed at the interface of LSM/TZ3Y. It has been found that the diffusion/dissolution of Mn ions in TZ3Y leads to the formation of the fluorite-type cubic zirconia solid solution, while the interaction of lanthanum with TZ3Y results in the formation of the lanthanum zirconate pyrochlore phase. Phase studies in the $(ZrY)O_2$–La_2O_3–Mn_3O_4 system show that the fluorite-type cubic zirconia solid solution phase c-$(Zr,Mn,La,Y)O_2$, rather than the tetragonal 3 mol% Y_2O_3–ZrO_2 phase, is in equilibrium with LSM perovskite at high temperatures. A ternary phase diagram of the system at the $(ZrY)O_2$-rich end at 1400 °C in air was proposed based on the experimental results. It is suggested that the fundamental reason for the beneficial effect of A-site non-stoichiometry or Mn excess of LSM in the inhibiting of the lanthanum zirconate formation is due to the fact that Mn_3O_4 does not equilibrate with lanthanum zirconate at high temperatures.

Keywords: Diffusion; Fuel cells; Interfaces; Perovskites; Phase diagram; ZrO_2; $(La,Sr)MnO_3$

1. Introduction

Strontium-doped lanthanum manganese oxide, $(LaSr)MnO_3$ (LSM), and yttria partially or fully stabilised zirconia, Y_2O_3–ZrO_2 or $(Zr,Y)O_2$, are commonly used as cathode and electrolyte materials respectively in solid oxide fuel cells (SOFC). Chemical interactions between LSM and yttria fully stabilised zirconia (e.g., 8 mol% Y_2O_3–ZrO_2) have been extensively studied due to the importance of the interfacial reaction and the formation of interfacial products on the performance and stability of SOFC under operation conditions.[1] The interfacial pyrochlore products of the chemical interaction vary with the stoichiometry of LSM,[2–4] the La/Sr ratio at the A-site[5,6] and the temperature and atmosphere of heat treatment.[7,8] The interfacial products formed, lanthanum zirconate $La_2Zr_2O_7$ and/or strontium zirconate $Sr_2Zr_2O_7$ are highly resistive and insulating, leading to interface delamination and deterioration in the fuel cell performance.[2,7,9,10] However, information on the interaction between LSM and partially stabilised zirconia such as 3 mol% Y_2O_3 tetragonal zirconia (TZ3Y) is limited, despite the fact that TZ3Y is of considerable interest to planar SOFC technology developers because of its high mechanical strength.

Roosmalen and Cordfunke[11] studied the interaction between TZ3Y and LSM dense pellets, and found that TZ3Y was more reactive than yttria fully stabilised zirconia (YSZ) in the formation of pyrochlore phase with LSM. Mn ions were not detected in the zirconia phase. Our previous study[12] on the interaction between strontium-doped praseodymium manganite (PSM) and 3 mol% yttria tetragonal zirconia (TZ3Y) shows that a fluorite-type phase of zirconia solid solution is formed between PSM and TZ3Y in addition to the formation of

* Corresponding author. Tel.: +65-6790-5010; fax: +65-6791-1859.
E-mail address: mspjiang@ntu.edu.sg (S. P. Jiang).

0955-2219/03/$ - see front matter © 2003 Elsevier Science Ltd. All rights reserved.
doi:10.1016/S0955-2219(02)00447-8

praseodymium zirconate. The formation of the fluorite-type cubic zirconia solid solution is due to the diffusion/dissolution of Mn ions into the tetragonal zirconia phase. Mn can diffuse into the tetragonal TZ3Y phase while Pr is most likely trapped by the formation of the praseodymium zirconate pyrochlore phase. Therefore it is important to investigate the chemical interactions between LSM and TZ3Y and the interfacial product formation in the LSM/TZ3Y system. In this paper, interfacial reactions between various diffusion couples of TZ3Y, LSM, lanthanum oxide and manganese oxide over the temperature range of 1300–1500 °C in air have been investigated, and the phase relations in the TZ3Y–La_2O_3–Mn_3O_4 system at the TZ3Y-rich end at 1400 °C in air are reported.

2. Experimental

LSM powder with composition $(La_{0.8}Sr_{0.2})MnO_3$ was prepared by wet chemical method and calcined at 1000 °C for 4 h in air. X-ray diffraction (XRD) pattern showed that the LSM powder was a single perovskite phase. TZ3Y substrates, 20 mm in diameter and 150 μm in thickness, were prepared from 3 mol% Y_2O_3–ZrO_2 (TZ3Y, Tosoh Corporation, Japan) by tape casting followed by sintering at 1500 °C. Powders of lanthanum oxide La_2O_3 (BDH, Analar grade) were calcined at 1000 °C for 2 h before use, and manganese oxide MnO_2 (BDH, chemical grade) without calcination treatment were used for solid state reaction. Inks of LSM, La_2O_3 and MnO_2 were prepared using Degussa water-based ink medium.

The diffusion couples of LSM/TZ3Y, La_2O_3/TZ3Y and MnO_2/TZ3Y were prepared by screen printing LSM, La_2O_3, and MnO_2 coatings on the TZ3Y substrate respectively, and then heat-treated at temperatures in the range of 1300–1500 °C for different times. The coating thickness was in the range of 40 to 50 μm thick. After heat treatments, the diffusion couples were carefully fractured and in some cases polished cross sections were prepared. A thermally-etched cross section of the specimen LSM/TZ3Y was also prepared by heating the polished cross section at 1500 °C for 5 min after the LSM coating was completely removed from the substrate to ensure no further chemical reaction between LSM and TZ3Y during the thermal etching process. In order to examine the surface morphology of TZ3Y substrates at the interface with coatings of LSM, lanthanum oxide and manganese oxide, the coatings were removed in various ways. LSM coating was removed relatively easily from the substrate after heat treatment at temperatures up to 1400 °C by a sharp doctor blade. The La_2O_3 film became powdery two days after heat treatment due to hydration of La_2O_3 in air and was then wiped off carefully using soft tissue. In the case of the MnO_2/TZ3Y diffusion couple, Mn_3O_4 was formed after the heat treatment at temperatures over 1000 °C.[13] This was removed by dissolving it in concentrated hydrochloric acid.

The fractured face, polished cross section and thermally etched cross section were examined with scanning electron microscopy (SEM) and X-ray energy dispersive spectroscopy (EDS). The surface of the TZ3Y substrate after removal of the oxide coatings was examined by XRD and SEM/EDS. A Siemens D500 X-ray diffractometer (Siemens, Germany) with CuK_α radiation and a Leica 360 field emission SEM (Cambridge, U.K.) equipped with Oxford Link EDS system were used for specimen characterization.

Powder experiments were also carried out to investigate the phase relations in the system TZ3Y–La_2O_3–Mn_3O_4 at the TZ3Y-rich end at 1400 °C. Powders of La_2O_3/TZ3Y, MnO_2/TZ3Y and La_2O_3/MnO_2/TZ3Y with various nominated mole ratios were mixed and milled in isopropyl alcohol for 2 h. The powder mixtures were pressed into pellets and then heated at 1400 °C for 24 h in air. Phase characterization of these samples was carried out by XRD and SEM/EDS.

3. Results

3.1. Reaction products in diffusion couples

The LSM/TZ3Y diffusion couples were heated at 1300, 1400 and 1500 °C for 4 h in air respectively. The LSM coatings were separated easily from the substrate after the heat treatment at 1300 and 1400 °C but adhered well on the substrate after the heat treatment at 1500 °C. Fig. 1 shows SEM pictures of (a) a fractured cross section of a specimen heat-treated at 1500 °C, and (b) a polished and thermally etched cross section of a specimen heat-treated at 1400 °C. Comparing to the typical tetragonal zirconia morphology in the TZ3Y bulk (marked as TZ3Y in the figure), it can be seen that two distinct reaction layers are formed between the LSM and TZ3Y phases, marked as "L1" and "L2" in Fig. 1. Reaction layer "L1" is the top surface layer in direct contact with the LSM coating and "L2" is the reaction layer between "L1" and the normal TZ3Y phase. Clearly, the grain size in the reaction layers "L1" and "L2" is much larger than that of the original TZ3Y phase.

Fig. 2 is the EDS spectra collected (a) from the first reaction layer "L1", and (b) the upper and (c) the lower parts of the second reaction layer "L2" of the specimen shown in Fig. 1b. A portion of these spectra from 13 to 19 keV was expanded on the Y-axis to show the K peaks associated with Sr and Y. It can be seen from Fig. 2 that the first reaction layer "L1" contains primary Zr and La and a small amount of Sr and Y. XRD analysis confirmed

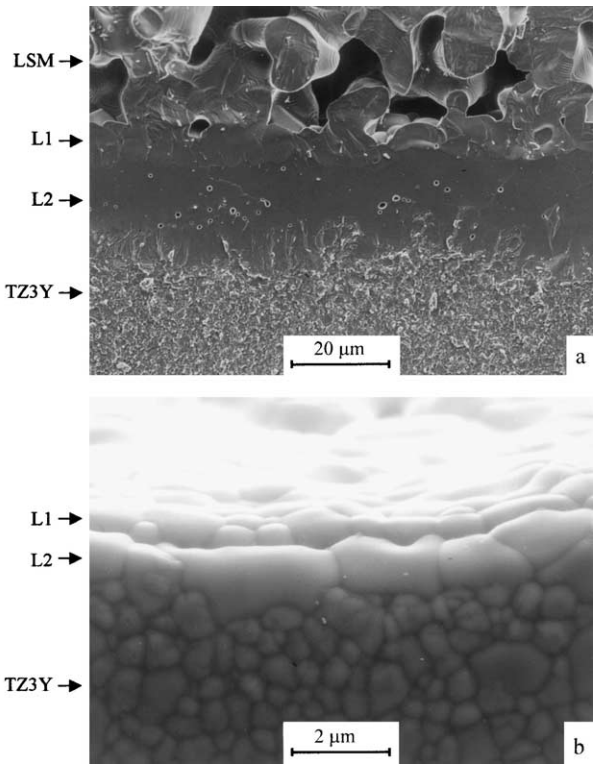

Fig. 1. SEM pictures taken from (a) a fractured cross section of the LSM/TZ3Y specimen after heat treatment at 1500 °C and (b) the polished and thermally etched cross section of the LSM/TZ3Y specimen after heat treatment at 1400 °C, showing the formation of two distinct reaction layers "L1" and "L2".

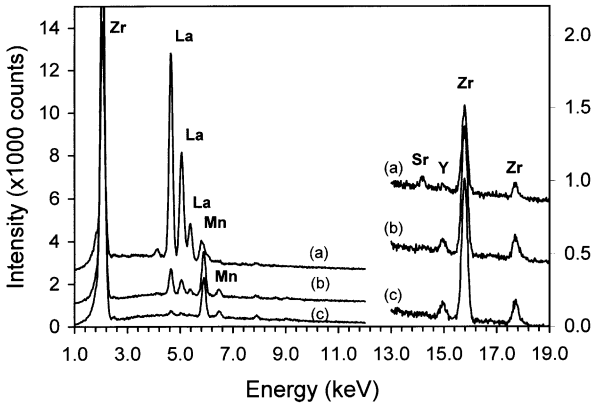

Fig. 2. The EDS spectra collected from (a) the first reaction layer "L1", (b) the upper part of the second reaction layer "L2″ and (c) the lower part of the second reaction layer "L2" of specimen of Fig.1b. A portion of these spectra from 13 to 19 keV was expanded in Y-axis to show the K peaks of Sr and Y.

the formation of a lanthanum/strontium zirconate pyrochlore phase with a possible composition of $(La,Sr)_2(Zr,Y)_2O_7$. In the second reaction layer "L2" Mn and La were detected in addition to Zr and Y, but no Sr was detected. This indicates that Mn and La ions diffused into TZ3Y. As shown in the following section, the results of powder experiments indicate that the La and Mn ions can dissolve in the zirconia lattice forming

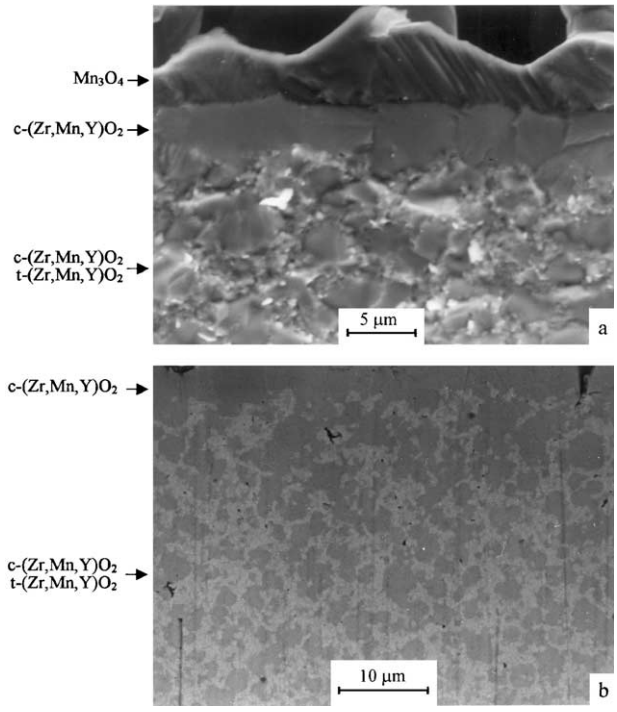

Fig. 3. SEM pictures of (a) fractured cross section and (b) polished cross section of the MnO_2/TZ3Y diffusion couple after heat treatment at 1300 °C for 24 h, showing a distinct reaction layer in the substrate next to Mn_3O_4 coating and a mixture of two types of materials in the substrate underneath the reaction layer.

a fluorite-type cubic zirconia solid solution $(Zr,Mn,La,Y)O_2$. Further away from the LSM/TZ3Y interface, primarily Mn was detected in the TZ3Y phase with very little La [curve (c) in Fig. 2]. The La concentration decreases significantly from the first reaction layer "L1" to the second reaction layer "L2", while the Mn concentration varied only slightly across the whole reaction layer, as shown in Fig. 2. Mn was also detected in the substrate below the second zirconia solid solution layer, but not La and Sr. The two reaction layers, $(La,Sr)_2(Zr,Y)_2O_7$ pyrochlore layer and cubic zirconia solid solution layer, were also observed in the LSM/TZ3Y specimen after heat treatment at 1300C. The formation of such two distinctive layers was also observed at the PSM/TZ3Y interface studied at temperature ranges of 1200–1400 °C.[12]

Fig. 3 shows SEM pictures of fractured and polished cross sections of a MnO_2/TZ3Y diffusion couple, showing a distinct reaction layer in the substrate next to the MnO_2 (or Mn_3O_4) coating. The MnO_2/TZ3Y diffusion couple was heated at 1300 °C for 24 h. After the heat treatment the TZ3Y substrate deformed slightly and became brittle. Mn as well as Zr and Y were detected in the reaction layer. XRD analysis on the substrate surface after removal of Mn_3O_4 by acid treatment showed a fluorite-type cubic zirconia solid solution phase, c-$(Zr,Mn,Y)O_2$. From the backscattered electron image of the polished cross section (Fig. 3b), it can be

seen that the substrate underneath the cubic zirconia solid solution layer is a mixture of two types of materials, characterised by the difference in the contrast. Fig. 4 is the EDS patterns collected from dark-contrast and bright-contrast areas of the reaction layers as shown in Fig. 3. EDS analysis showed that the dark-contrast material contained significant amount of Mn (see Fig. 4a) whereas the level of Mn in the bright-contrast material is much lower (Fig. 4b). Detailed XRD analysis showed that the dark-contrast materials were cubic zirconia phase with c-$(Zr,Mn,Y)O_2$ composition and the bright-contrast materials had the same structure as TZ3Y with much lower level of Mn dissolved in it. Mn was also detected by EDS from the other side of TZ3Y, indicating that Mn diffused through the TZ3Y substrate (the thickness of the TZ3Y substrate was about 150 μm). Mn concentration in the substrate decreased with the increase of the distance from the manganese oxide coating contact surface.

Fig. 5 shows SEM pictures of the surface of a zirconia substrate after removal of manganese oxide by acid washing treatment and the original TZ3Y surface before the heat treatment at 1300 °C. The grain size of TZ3Y before the chemical interaction with manganese oxide was 0.4 μm in average. After heat treatment of the MnO_2/TZ3Y diffusion couple, the zirconia grain size was in the range of 3–12 μm, significantly larger than the original TZ3Y grains. Clearly Mn ions have dissolved in zirconia, leading to the significant grain growth and the phase transformation from tetragonal zirconia to cubic zirocnia, as identified by XRD. As shown by Waller et al. the diffusion coefficient of manganese in polycrystalline YSZ is much higher than that in single crystal YSZ.[14] This indicates that the diffusion/dissolution of Mn ions in polycrystalline TZ3Y is dominated by the grain boundary diffusion. Hence the formation of the fluorite-type cubic zirconia solid solution would start at the original TZ3Y grain boundary region. The grain growth of the fluorite-type cubic zirconia

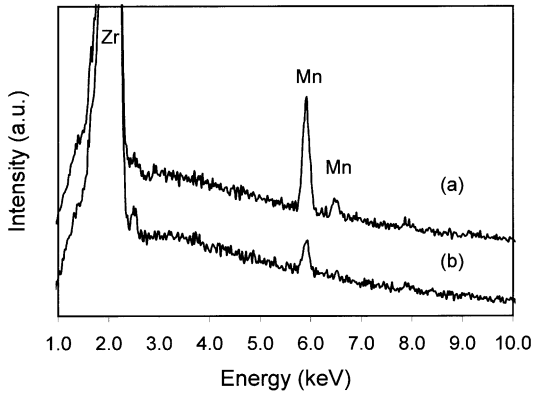

Fig. 4. EDS spectra collected from (a) the dark-contrast material and (b) the bright-contrast material as shown in Fig. 3(b), showing the difference in Mn concentration between these two materials.

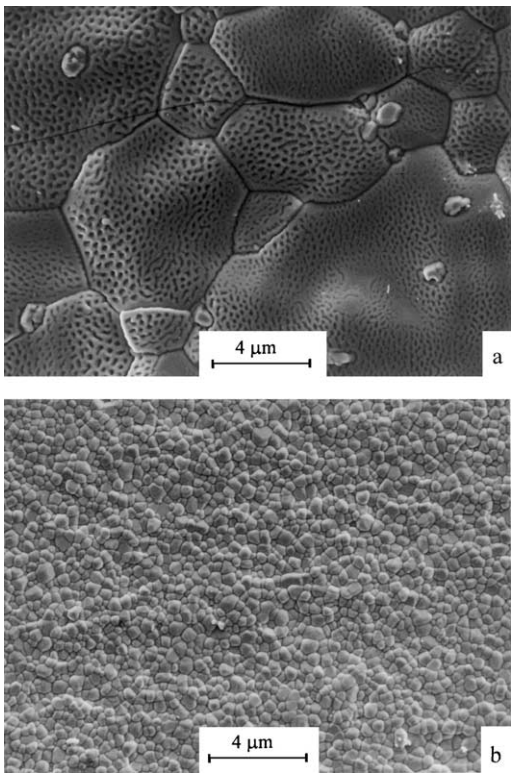

Fig. 5. SEM pictures from (a) the surface of fluorite-type zirconia solid solution after removal of manganese oxide by acid washing and (b) the surface of the TZ3Y before the reaction. The MnO_2/TZ3Y diffusion couple was heated at 1300 °C for 24 h in air.

phase significantly reduced the number of original much smaller tetragonal zirconia grains. Many small pores were also observed on the grain surface of the zirconia electrolyte surface. However, in the case of LSM/TZ3Y specimen, there was no formation of small pores on the grain surface of cubic zirconia solid solution formed (Fig. 1). Similarly no small pore formation was found on the grain surface of PSM/TZ3Y specimen.[12] At this stage it is not clear for the reason of the formation of micropores on the zirconia surface in the case of MnO_2/TZ3Y specimen (see Fig. 5a). The results of the MnO_2/TZ3Y diffusion couple experiments demonstrate that the diffusion/dissolution of significant amount of Mn in TZ3Y is responsible for the formation of the fluorite-type cubic zirconia solid solution and significantly changes the surface morphology of the substrate.

The effect of diffusion/dissolution of La ions in TZ3Y on interface product formation was examined on the La_2O_3/TZ3Y diffusion couples. The La_2O_3/TZ3Y diffusion couples were heated for 24 h at 1300 and 1400 °C in air respectively. In both cases a continuous reaction layer was formed between La_2O_3 and TZ3Y. For the La_2O_3/TZ3Y diffusion couple after heat treatment at 1300 °C for 24 h, the thickness of the continuous reaction layer was about 1 μm. XRD and EDS analysis indicate that the reaction layer is essentially the lanthanum zirconate pyrochlore phase ($La_2Zr_2O_7$). No other

reaction layer or phases except tetragonal TZ3Y phase were detected. This is consistent with the interface studies of the La_2O_3 on YSZ single crystals at 1500 °C.[10] However, the formation of lanthanum zirconate containing small amount of yttria cannot be ruled out as it would be difficulty to distinguish these two phases by using XRD and EDS only. La was not detected in the TZ3Y phase underneath the pyrochlore reaction layer. The results of the La_2O_3/TZ3Y diffusion couples have shown that the interaction of La ions and TZ3Y alone will result in the formation of lanthanum zirconate pyrochlore, but not the fluorite-type cubic zirconia solid solution. The clear La content boundary between the lanthanum zirconate pyrochlore phase and TZ3Y phase also suggests that unlike Mn, La hardly dissolves or diffuses in the tetragonal zirconia phase and the solubility of La in TZ3Y is negligible.

An experiment was designed to study the diffusion/dissolution of both Mn and La ions in TZ3Y. First, a La_2O_3/TZ3Y diffusion couple was heated at 1300 °C for 24 h to form a pyrochlore layer on the TZ3Y surface. Then excess La_2O_3 coating was removed and MnO_2 coating was screen printed on top of the pyrochlore layer. As shown above, for the La_2O_3/TZ3Y diffusion couple treated at 1300 °C for 24 h, the thickness of the lanthanum zirconate pyrochlore layer was ~1 μm. The prepared specimen with structure of MnO_2/pyrochlore/TZ3Y was heated again at 1300 °C for 24 h in air. SEM/EDS analysis of this specimen after heat treatment showed that the original lanthanum zirconate pyrochlore layer (ca. 1 μm thick) completely disappeared from the interface region and cubic zirconia solid solution was formed instead. La ions originally in the pyrochlore phase have dissolved in the cubic zirconia solid solution formed due to the dissolution of Mn ions. Fig. 6 is the energy dispersive X-ray line scan traces recorded over a line across the interface showing the distribution of the major elements Zr, La and Mn across the interface. The thickness of the cubic zirconia solid solution $(Zr,Mn,La,Y)O_2$ layer was ~5 μm thick, significantly higher than that of the original pyrochlore reaction layer (~1 μm). The results of this test show that, when the amount of Mn ions is much higher than that of La ions in the region of interface with TZ3Y, the interfacial reaction would be dominated by the Mn diffusion and subsequently the formation of fluorite-type cubic zirconia solid solution. This is followed by the diffusion/dissolution of La in the fluorite-type cubic zirconia solid solution formed. In conclusion, Mn_3O_4 cannot be in equilibrium with lanthanum zirconate pyrochlore phase at high temperatures. This may be the fundamental reason for the observations that A-site non-stoichiometry or A-site deficient in LSM is beneficial for the inhibiting of the formation of lanthanum zirconate at the LSM/YSZ interface.[2,4,5,9,15]

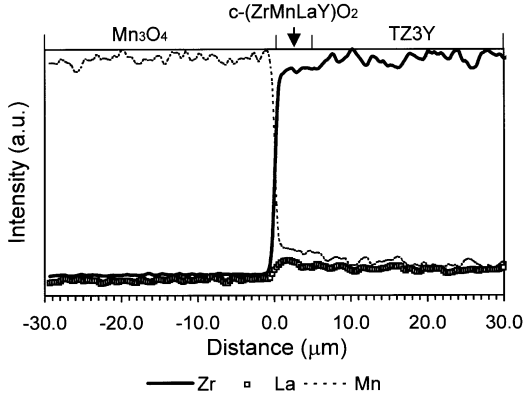

Fig. 6. The energy dispersive X-ray line scan traces recorded over a line across the interface of the triple layer specimen, MnO_2/pyrochlore/TZ3Y, after heat treatment at 1300 °C for 24 h, showing the distribution of the major elements Zr, La and Mn along the line.

3.2. Reaction products in powder mixtures

Powder experiments on La_2O_3/TZ3Y, MnO_2/TZ3Y and La_2O_3/MnO_2/TZ3Y with various compositions were carried out. The compositions of the powder mixtures and the phases of the products after 24 h at 1400 °C are listed in Table 1. Lanthanum zirconate pyrochlore ($La_2Zr_2O_7$) phase was formed between TZ3Y and La_2O_3 in the composition range studied. No other phases were identified in the La_2O_3/TZ3Y powder mixtures except the un-reacted tetragonal TZ3Y phase. This again confirms that lanthanum does not dissolve in the tetragonal zirconia phase. On the other hand, manganese oxide reacted with the tetragonal TZ3Y at 1400 °C, forming mixed phases of tetragonal zirconia phase and fluorite-type cubic zirconia solid solution

Table 1
Compositions and phases of powder mixture of various diffusion couples after heat treatment at 1400 °C for 24 h in air

Compositions	Phases
$(TZ3Y)_{0.95}(1/2\ La_2O_3)_{0.05}$	t-$(Zr,Y)O_2$, $La_2(Zr,Y)_2O_7$
$(TZ3Y)_{0.90}(1/2\ La_2O_3)_{0.10}$	t-$(Zr,Y)O_2$, $La_2(Zr,Y)_2O_7$
$(TZ3Y)_{0.80}(112\ La_2O_3)_{0.20}$	t-$(Zr,Y)O_2$, $La_2(Zr,Y)_2O_7$
$(TZ3Y)_{0.97}(MnO_2)_{0.03}$	c-$(Zr,Mn,Y)O_2$, t-$(Zr,Mn,Y)O_2$
$(TZ3Y)_{0.94}(MnO_2)_{0.06}$	c-$(Zr,Mn,Y)O_2$, t-$(Zr,Mn,Y)O_2$
$(TZ3Y)_{0.91}(MnO_2)_{0.09}$	c-$(Zr,Mn,Y)O_2$, t-$(Zr,Mn,Y)O_2$
$(TZ3Y)_{0.85}(Mn0_2)_{0.15}$	c-$(Zr,Mn,Y)O_2$
$(TZ3Y)_{0.75}(Mn0_2)_{0.25}$	c-$(Zr,Mn,Y)O_2$, Mn_3O_4
$(TZ3Y)_{0.90}(1/2\ La_2O_3)_{0.04}(MnO_2)_{0.06}$	c-$(Zr,Mn,La,Y)O_2$, t-$(Zr,Mn,La,Y)O_2$, $La_2(Zr,Y)_2O_7$
$(TZ3Y)_{0.80}(1/2\ La_2O_3)_{0.08}(MnO_2)_{0.12}$	c-$(Zr,Mn,La,Y)O_2$, $La_2(Zr,Y)_2O_7$
$(TZ3Y)_{0.65}(1/2\ La_2O_3)_{0.14}(Mn0_2)_{0.21}$	c-$(Zr,Mn,La,Y)O_2$, $La_2(Zr,Y)_2O_7$, $LaMnO_3$
$(TZ3Y)_{0.45}(1/2\ La_2O_3)_{0.22}(MnO_2)_{0.33}$	c-$(Zr,Mn,La,Y)O_2$, $LaMnO_3$
$(TZ3Y)_{0.76}(1/2\ La_2O_3)_{0.04}(MnO_2)_{0.20}$	c-$(Zr,Mn,La,Y)O_2$

"t" Denotes the tetragonal zirconia phase. "c" Denotes the cubic zirconia phase.

with Mn and Y ions dissolved in it. SEM examination showed mixed phases of dark- and bright-contrast phases, similar to that shown in Fig. 3b. When the MnO_2 concentration was higher than 15 mol%, EDS analysis only detected fluorite-type cubic zirconia phase. Fig. 7 shows the XRD patterns of the tetragonal TZ3Y and the reaction product of $(TZ3Y)_{0.85}(MnO_2)_{0.15}$ after the heat treatment at 1400 °C for 24 h. It can be seen that the peaks of the tetragonal zirconia phase have disappeared from the XRD trace of the product. All reflections of the XRD patterns of Fig. 7b belong to the phase of fluorite-type cubic zirconia solid solution, c-$(Zr,Mn,Y)O_2$, indicating the complete reaction of MnO_2 with TZ3Y phase. When the mole ratio of MnO_2/TZ3Y increased to 0.25/0.75, a small amount of Mn_3O_4 was detected in addition to the c-$(Zr,Mn,Y)O_2$ phase. This indicates that the solubility limit of Mn ions in the cubic zirconia solid solution phase lies between 15 and 25 mol%.

In the case of the powder mixture experiments of La_2O_3/MnO_2/TZ3Y, the phase formation is more complicated, depending on both Mn/La and Mn/TZ3Y ratios. The fluorite-type zirconia solid solution, c-$(Zr,Mn,La,Y)O_2$, identified by XRD and SEM/EDS, was formed in all the compositions studied. As shown early, the solubility of Mn ions in tetragonal phase of zirconia is less than 3 mol%.[12] Thus fluorite-type zirconia solid solution would form when the Mn concentration in tetragonal zirconia phase is higher than 3 mol%. However, the formation of other phases is dependent on the MnO_2 content and the (Mn/La)/TZ3Y ratios in the mixture. In the first four La_2O_3/MnO_2/TZ3Y diffusion couples, the mole ratio of Mn/La was kept the same as 1.5 (see Table 1). When the concentration of TZ3Y was high (e.g., 90 mol%), $La_2Zr_2O_7$ and c-$(Zr,Mn,La,Y)O_2$ phases were formed in addition to the unreacted TZ3Y. When the concentration of TZ3Y was decreased to 80 mol%, $La_2Zr_2O_7$ was formed in addition to the c-$(Zr,Mn,La,Y)O_2$ with the complete disappearance of original tetragonal zirconia phase. With the further reduction in the concentration of TZ3Y to 65 mol%, $LaMnO_3$ was formed in addition to $La_2Zr_2O_7$ and c-$(Zr,Mn,La,Y)O_2$ phases. As the content of TZ3Y decreased to 45 mol%, $LaMnO_3$ became the major phase in the reaction products in addition to the fluorite-type cubic zirconia solid solution c-$(Zr,Mn,La,Y)O_2$. Moreover, the pyrochlore phase $La_2Zr_2O_7$ was not detected at this composition. A few Mn_3O_4 grains were observed by SEM/EDS in this case, indicating the excess of manganese oxide. This indicates that excess of manganese will inhibit the formation of $La_2Zr_2O_7$ phase. This is further supported by the fact when the Ma/La ratio increased to 5 ($(TZ3Y)_{0.76}(1/2\ La_2O_3)_{0.04}(MnO_2)_{0.20}$ diffusion couple), pyrochlore phase $La_2Zr_2O_7$ was not detected and the only product was the fluorite-type cubic zirconia solid solution c-$(Zr,Mn,La,Y)O_2$.

Fig. 8 is the ternary phase diagram of $(Zr,Y)O_2$–La_2O_3–Mn_3O_4 system at 1400 °C in air based on the powder mixture experiments. Symbols "+" are the experimental data based on the powder experiments. In the diagram, $(Zr,Y)O_2$ represents the 3mol% Y_2O_3–ZrO_2 (TZ3Y) phase and La_yMnO_3 represents the perovskite phase due to its non-stoichiometry on the A-site.[16] However, the detailed identification of the La_yMnO_3 perovskite phase was not carried out in this study. The existence of a narrow tetragonal zirconia solid solution t-$(Zr,Mn,La,Y)O_2$ region is based on the observation of the mixed tetragonal zirocnia and cubic zirconia phases in the low concentration of MnO_2 (or

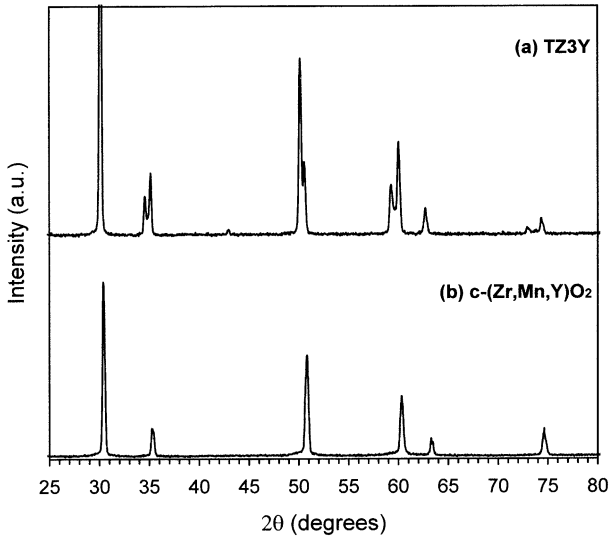

Fig. 7. XRD patterns of (a) the tetragonal TZ3Y powder and (b) the reaction product of $(TZ3Y)_{0.85}(MnO_2)_{0.15}$ after heat treatment at 1400 °C for 24 h, showing the disappearance of the tetragonal zirconia phase and the formation of a fluorite-type cubic zirconia solid solution phase.

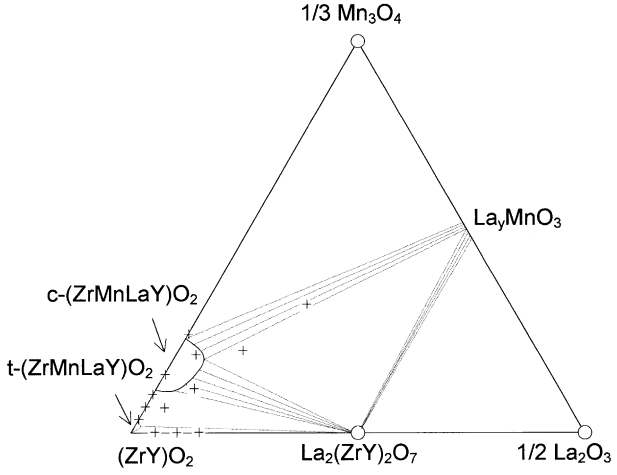

Fig. 8. Ternary phase diagram of $(ZrY)O_2$–La_2O_3–Mn_3O_4 system at 1400 °C in air. $(ZrY)O_2$ denotes 3 mol% Y_2O_3-ZrO_2. Symbols "+" are the experimental data.

Mn_3O_4), indicated by the co-existence of dark- and bright-contrast zirconia phases (Fig. 3b). According to the phase diagram, some important phase relations can be drawn out as follows:

1. TZ3Y phase and La_yMnO_3 perovskite phase can not be in equilibrium with each other at 1400 °C in air.
2. Mn_3O_4 and $La_2Zr_2O_7$ pyrochlore phase can not be in equilibrium with each other at 1400 °C in air.
3. On the other hand, the fluorite-type cubic zirconia solid solution c-(Zr,Mn,La,Y)O_2 can be in equilibrium with pyrochlore phase, perovskite phase and manganese oxide, respectively.

4. Discussion

The interaction between tetragonal TZ3Y and LSM perovskite at high temperatures resulted in the formation of two distinct reaction layers, the fluorite-type cubic zirconia solid solution layer and the lanthanum zirconate pyrochlore layer. This is very different from the results of the chemical interaction between fully stablised zirconia (YSZ) phase and LSM perovskite where only one reaction layer of pyrochlore phase was formed although the diffusion of Mn and La ions into zirconia was observed.[17–19] This is due to the fact that YSZ is a fluorite-type cubic phase by itself. Thus the diffusion/dissolution of Mn and La ions will not change the fluorite-type cubic structure that is already existed.

From the present studies, it is clear that the diffusion/dissolution of the Mn ions from LSM into TZ3Y is responsible for the formation of the fluorite-type cubic zirconia solid solution c-(Zr,Mn,La,Y)O_2, while the interaction of La with TZ3Y is responsible for the formation of the pyrochlore phase $La_2Zr_2O_7$. It is known that Mn ions are soluble to some extent in 3 mol% Y_2O_3-ZrO_2 (e.g., up to 3 mol% Mn in TZ3Y), leading to the formation of the tetragonal zirconia solid solution t-(Zr,Mn,Y)O_2, as shown in Fig. 3b. Further increase of Mn ion concentration will cause the phase transformation from tetragonal to fluorite-type cubic zirconia solid solution. However, when La ions alone diffused into TZ3Y at temperature range of 1300–1500 °C, lanthanum zirconate pyrochlore phase instead of fluorite-type cubic zirconia phase was formed. This is consistent with the phase diagram of La_2O_3–ZrO_2 reported by Brown et al.[20] La was not detected in the TZ3Y phase, indicating that the solubility of La ions in the tetragonal zirconia phase is small. In the presence of Mn and La ions, the diffusion of Mn would be a dominant process, forming preferentially the fluorite-type cubic zirconia phase. This would be followed by the diffusion/dissolution of La in the cubic zirconia phase c-(Zr,Mn,Y)O_2, forming the solid solution c-(Zr,Mn,La,Y)O_2 and pyrochlore phase $La_2Zr_2O_7$ at the LSM/TZ3Y interface if the La concentration is higher than the solubility limit of La in the cubic zirconia phase. The formation of the fluorite-type cubic zirconia phase c-(Zr,Mn,La,Y)O_2 in the La_2O_3/MnO_2/TZ3Y system but not in the La_2O_3/TZ3Y system indicates that La can diffuse into fluorite-type cubic zirconia phase but not the tetragonal zirconia phase.

The powder experiments not only confirmed the results obtained from the diffusion couple experiments, but also revealed the phase relations among the components involved in the chemical interaction at the LSM/TZ3Y interface. With the help of the phase diagram (see Fig. 8), the driving force for the formation of the fluorite-type zirconia solid solution and the pyrochlore phase between LSM and TZ3Y can be explained. The diffusion couple of LSM/TZ3Y is a non-equilibrium system at 1400 °C in air and thus is not stable. In order to reach the equilibrium state of the fluorite-type cubic zirconia solid solution/pyrochlore/perovskite, Mn and La ions have to diffuse through the interface and react with TZ3Y to form the fluorite-type cubic zirconia solid solution and the lanthanum zirconate pyrochlore phase. However, once a continuous reaction layer is formed, the LSM coating and TZ3Y substrate are separated by this reaction layer, and the reaction rate would decrease significantly. If the concentration of Mn ions is much higher than that of La ions in the interface region with TZ3Y, the formation of lanthanum zirconate pyrochlore phase will be depressed and instead there will be preferential formation of $LaMnO_3$ perovskite phase. This is confirmed by the results of the MnO_2/$La_2Zr_2O_7$ pyrochlore/TZ3Y experiment. The reasons are that the lanthanum zirconate pyrochlore phase cannot be in equilibrium with Mn_3O_4 at high temperatures according to the phase diagram of Fig. 8.

The phase diagram obtained in the present study agrees in general with the theoretical phase diagram of ZrO_2–La_2O_3–Mn_3O_4 system at 1300 °C reported by Yokokawa et al.[8] The major difference between the present experimental and theoretical phase diagrams is in the size and position of the zirconia solid solution region. The maximum Mn solubility in the zirconia solid solution determined in the present study is almost twice that determined from the theoretically calculated phase diagram. Kuscer et al.[21] reported a ternary phase diagram for the ZrO_2–La_2O_3–Mn_3O_4 system at 1450 °C in which they drew a tie line between Mn_2O_3 (it should be Mn_3O_4 at 1450C) and $La_2Zr_2O_7$, suggesting that manganese oxide could be formed together with the pyrochlore phase when $LaMnO_3$ reacts with ZrO_2. The present study has shown that Mn_3O_4 and pyrochlore phase $La_2Zr_2O_7$ cannot be in equilibrium with each other at high temperatures (e.g., 1400 °C or higher) in

air. The equilibrium reaction products between $LaMnO_3$ and ZrO_2 are the cubic zirconia phase and the pyrochlore phase.

The formation of the pyrochlore phase at the LSM electrode and zirconia electrolyte interface has significant detrimental effect on the electrochemical performance of SOFC.[2,9,22] However, it is well known that lanthanum zirconate pyrochlore phase formation can be depressed by using an A-site non-stoichiometrical composition of LSM perovskite.[2–4] This is confirmed by the present studies on the phase formation in the TZ3Y/La_2O_3/MnO_2 powder mixtures and the MnO_2/$La_2Zr_2O_7$ pyrochlore/TZ3Y diffusion couple. Excess manganese would depress the formation of lanthanum zirconate pyrochlore in the LSM/zirconia system. As for fluorite-type zirconia solid solution containing Mn and La ions, the phase diagram has shown that the lanthanum zirconate pyrochlore phase would be formed eventually regardless of the starting stoichiometry composition of the LSM perovskite. In SOFC based on TZ3Y electrolyte system, the formation of a fluorite-type cubic zirconia solid solution layer would reduce the mechanical strength and make the electrolyte relatively brittle, due to the low mechanical strength of cubic zirconia compared to tetragonal zirconia. On the other hand, cubic zirconia phase has much larger grain size as compared to that of tetragonal zirconia (Fig. 1) and the ionic conductivity of cubic zirconia such as 8 mol% Y_2O_3–ZrO_2 is higher by a factor of about three compared with tetragonal zirconia at 1000 °C.[23] However, the effect of the formation of the fluorite-type zirconia solid solution layer at the LSM/TZ3Y interface on the electrochemical performance is not clear at this stage. The chemical interaction between LSM and TZ3Y at SOFC operating temperature range (800–1000 °C) may not be significant in a short term as the diffusion of La and Mn ions from the LSM perovskite to the TZ3Y phase would be much slower at 800–1000 °C than that at 1400 °C. Nevertheless, the formation of very thin reaction layers of fluorite-type cubic zirconia solid solution and lanthanum zirconate pyrochlore at the LSM/TZ3Y interface could be detrimental to the long term performance and stability of the fuel cells particularly for SOFC based on thin-film electrolytes.

5. Conclusions

The interaction between $(La_{0.8}Sr_{0.2})MnO_3$ and TZ3Y has been studied at temperature range 1300–1500 °C. Two distinct reaction layers, fluorite-type cubic zirconia solid solution and lanthanum zirconate pyrochlore phase were formed at the interface of LSM/TZ3Y, similar to that observed in the PSM/TZ3Y system.[12] The experiments on various diffusion couples between La_2O_3, MnO_2 and TZ3Y indicate that the formation of the fluorite-type zirconia phase is mainly due to the dissolution of Mn ions into TZ3Y, while the interaction of La ions with TZ3Y causes the formation of lanthanum zirconate pyrochlore phase. However, excess Mn would significantly depress the formation of $La_2Zr_2O_7$ phase. The phase relations among the components involved at the LSM/TZ3Y interface showed that the tetragonal TZ3Y cannot be in equilibrium with LSM perovskite at high temperatures (e.g., at 1400 °C). On the other hand, fluorite-type cubic zirconia solid solution phase, c-(Zr,Mn,La,Y)O_2, can be in equilibrium with the LSM perovskite phase. Thus from the phase stability point of view, 3 mol% Y_2O_3 tetragonal zirconia may not be an optimum choice as electrolyte materials in SOFC.

Acknowledgements

The authors are grateful to Mr. D. Milosevic, Mr. J. Baigent, Natasha Rockelmann and Kylie Chapman for their technical assistance.

References

1. Minh, N. Q., Ceramic fuel cells. *J. Am. Ceram. Soc.*, 1993, **76**(3), 563–588.
2. Jiang, S. P., Love, J. G., Zhang, J. P., Hoang, M., Ramprakash, Y., Hughes, A. E. and Badwal, S. P. S., The electrochemical performance of LSM/zirconia-yttria as a function of A-site non-stoichiometry and cathodic current treatment. *Solid State Ionics*, 1999, **121**, 1–10.
3. Tsepin, T. and Barnett, S. A., Effect of LSM-TZ3Y cathode on thin-electrolyte solid oxide fuel cell performance. *Solid State Ionics*, 1997, **93**, 207–217.
4. Mitterdorfer, A., Cantoni, M. and Gauckler, L. J., Interface formation between yttria-stabilized zirconia and porous $La_{0.85}Sr_{0.15}Mn_yO_3$ during firing at intermediate temperatures. In *Second European Solid Oxide Fuel Cells Forum*, ed. B. Thorstensen. European Fuel Cell Group, Lucerne, Switzerland, 1996, pp. 373–382.
5. Stchniol, G., Syskakis, E. and Naoumidis, A., Chemical compatibility between strontium-doped lanthanum manganite and yttria-stabilized zirconia. *J. Am. Ceram. Soc.*, 1995, **78**(4), 929–932.
6. Stochniol, G., Grubmeier, H., Naoumidis, A. and Nickel, H., EPMA on interfaces between cathode and electrolyte of the solid oxide fuel cell. In *Proceedings of the Fourth International Symposium on Solid Oxide Fuel Cells (SOFC-IV)*, ed. M. Dokiya, O. Yamamoto, H. Tagawa and S. C. Singhal. The Electrochemical Society, Pennington, NJ, 1995, pp. 995–1005.
7. Brugnoni, C., Ducati, U. and Scagliotti, M., SOFC cathode / electrolyte interface. Part I: Reactivity between $La_{0.85}Sr_{0.15}MnO_3$ and ZrO_2–Y_2O_3. *Solid State Ionics*, 1995, **76**, 177 –182.
8. Yokokawa, H., Sakai, N., Kawada, T. and Dokiya, M., Chemical thermodynamic stabilities of the interface. In *Science and Technology of Zirconia V*, ed. S. P. S. Badwal, M. J. Bannister and R. H. J. Hannink. Technomic Publishing Company, Inc, Lancaster, Pennsylvania, 1993, pp. 752–763.
9. Jiang, S. P., Zhang, J. P., Ramprakash, Y., Milosevic, D. and Wilshier, K., An investigation of shelf-life of strontium doped $LaMnO_3$ materials. *J. Mater. Sci.*, 2000, **35**, 2735–2741.
10. Chiodelli, G. and Scagliotti, M., Electrical characterization of

lanthanum zirconate reaction layers by impedance spectroscopy. *Solid State Ionics*, 1994, **73**, 265–271.
11. van Roosmalen, J. A. M. and Cordfunke, E. H. P., Chemical reactivity and interdiffusion of (La,Sr)Mno_3 and $(Zr,Y)O_2$, solid oxide fuel cell cathode and electrolyte materials. *Solid State Ionics*, 1992, **52**, 303–312.
12. Zhang, J.-P., Jiang, S. P., Love, J. G., Föger, K. and Badwal, S. P. S., Chemical interactions between strontium-doped praseodymium manganite and 3 mol% yttria-zirconia. *J. Mater. Chem.*, 1998, **8**, 2787–2794.
13. Klingsberg, C. and Roy, R., Solid –solid and solid–vapor reactions and a new phase in the system Mn-O. *J. Am. Ceram. Soc.*, 1992, **43**(12), 620–626.
14. Waller, D., Sirman, J. D. and Kilner, J. A., Manganese diffusion in single crytal and polycrystalline yttria stabilised zirconia. In *Proceedings of the Fifth International Symposium on Solid Oxide Fuel Cells (SOFC-V)*, ed. U. Stimming, S. C. Singhal, H. Tagawa and W. Lehnert. The Electrochemical Society, Pennington, NJ, 1997, pp. 1140–1149.
15. Mitterdorfer, A. and Gauckler, L. J., $La_2Zr_2O_7$ formation and oxygen reduction kinetics of the $La_{0.85}Sr_{0.15}Mn_yO_3$, O_2 (g)|YSZ system. *Solid State Ionics*, 1998, **111**, 185–218.
16. Yokokawa, H., Horita, T., Sakai, N., Dokiya, M. and Kawada, T., Thermodynamic representation of nonstoichiometric lanthanum manganite. *Solid State Ionics*, 1996, **8688**, 1161–1165.
17. Lau, S.K. and Singhal, S.C., Potential electrode/electrolyte interactions in solid oxide fuel cells. In *Corrosion 85*. National Association of Corrosion Engineers, Houston, TX, 1985, pp. 345/1-9.
18. Khandkar, A., Elangovan, S. and Liu, M., Materials considerations for application to solid state electrochemical devices. *Solid State Ionics*, 1992, **52**, 57–68.
19. Taimatsu, H., Wada, K. and Kaneko, H., Mechanism of reaction between lanthanum manganite and yttria-stabilized zirconia. *J. Am. Ceram. Soc.*, 1992, **75**(2), 401–405.
20. Brown, F. H. Jr. and Duwez, P., The systems zirconia-lanthanum and zirconia-neodymia. *J. Am. Ceram. Soc.*, 1955, **38**, 95–101.
21. Kuscer, D., Holc, J., Hrovat, M., Bernik, S., Samardzija, Z. and Kolar, D., Interactions between a thick film $LaMnO_3$ cathode and YSZ SOFC electrolyte during high temperature ageing. *Solid State Ionics*, 1995, **78**, 79–85.
22. Lee, H. Y. and Oh, S. M., Origin of cathodic degradation and new phase formation at the $La_{0.9}Sr_{0.1}MnO_3$ / TZ3Y interface. *Solid State Ionics*, 1996, **90**, 133–140.
23. Ciacchi, F. T., Crane, K. M. and Badwal, S. P. S., Evaluation of commercial zirconia powders for solid oxide fuel cells. *Solid State Ionics*, 1994, **73**, 49–61.